



Degradation of Orange II by electrochemical activation of persulfate: performance and mechanism

Shumin Zhu^a, Shiqing Zhou^b, Yanghai Yu^b, Naiyun Gao^a, Bingzhi Dong^{a,*}

^aState Key Laboratory of Pollution Control and Resource Reuse, College of Environmental Science and Engineering, Tongji University, Shanghai 200092, China, Tel. +86 21 65982691; email: dbzwater@163.com (B. Dong)

^bDepartment of Water Engineering and Science, College of Civil Engineering, Hunan University, Changsha, Hunan 410082, China

Received 11 December 2016; Accepted 26 August 2017

ABSTRACT

In this study, the degradation of Acid Orange II (AO II) by electrochemical activation of persulfate was systematically investigated. Iron electrode as the source of Fe^{2+} was verified to be the efficient activator for persulfate to produce sulfate radicals, which exhibited promising ability to degrade AO II than persulfate and electrocoagulation process. Compared with the addition of Fe^{2+} directly, the removal rates of AO II in the EC/PS system were almost twice of those in the Fe^{2+} /PS system at all the applied currents. The application of radical scavenger confirmed that both $\text{SO}_4^{\cdot-}$ and OH^{\cdot} existed in the EC/PS system and $\text{SO}_4^{\cdot-}$ is the predominant radical species for AO II degradation. Furthermore, increasing the applied current, persulfate concentration and reaction temperature improved the removal of AO II. The comparison of UV–visible spectrum demonstrated that the azo double bond in the AO II structure was destroyed efficiently and under current control in the EC/PS system. Finally, the degradation pathway was proposed in this study based on the results of gas chromatography–mass spectrometry (GC–MS).

Keywords: Electrochemical activation; Sulfate radical; Acid Orange II; Ferrous ions

1. Introduction

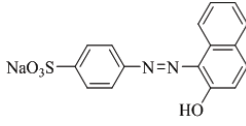
With the developing of printing and dyeing industry, different kinds of synthetic dyes were discharged into wastewater and environmental waters. Among these dyes, synthetic azo dyes constitute more than 50% of the dye production in the world [1], which were characterized by their high color and toxicities. Therefore, the removal of azo dyes from water has aroused great concern. Nevertheless, azo dyes always have stable structure, which contain one or more azo bonds ($-\text{N}=\text{N}-$) as chromophore group and aromatic structures associated with other functional groups. Acid Orange II (AO II; Table 1) is one of the most commonly found azo dyes in wastewater, which can remain in the ecosystem for decades and produce carcinogenic aromatic amines under certain conditions [2,3]. Although various traditional methods such

as coagulation, adsorption and biological treatments have been proposed for the removal of azo dyes from aqueous solutions, none of these treatments was satisfactory [4–6].

Advanced oxidation processes (AOPs) are effective toward degradation of a number of azo dyes [7–9], mainly based on hydroxyl radical (HO^{\cdot}) or sulfate radical ($\text{SO}_4^{\cdot-}$). HO^{\cdot} must be generated continuously in reactions as a consequence of its instability. $\text{SO}_4^{\cdot-}$ have a longer half life than HO^{\cdot} because of their preference for electron transfer reaction, while HO^{\cdot} can participate in a diversity of reaction with equal preference [10,11]. $\text{SO}_4^{\cdot-}$ are usually generated during the activation of persulfate (PS) or peroxymonosulfate by heat, UV, ultrasound or transition metals [12–15]. Among the transition metals, Fe^{2+} has been widely used to activate PS via Eq. (1) [16], since it is relatively inexpensive, nontoxic and effective [17]. However, direct addition of Fe^{2+} may lead to the decline of oxidation efficiency [15], because excessive Fe^{2+} can act as a scavenger of $\text{SO}_4^{\cdot-}$ via Eq. (2).

* Corresponding author.

Table 1
Selected physicochemical properties of Acid Orange II

Name	Acronym	Formula	Molecular weight	Structure
Acid Orange II	AO II	C ₁₆ H ₁₁ N ₂ SO ₄ Na	350.33	



In this work, electrochemical activation of persulfate (EC/PS) is a combination of electrochemistry (EC) and AOP, which takes advantages of both Fe²⁺ and SO₄^{·-}. Fe²⁺ is released from a sacrificial iron electrode continuously under direct current (DC), which not only acts as an activator of persulfate but also ultimately form ferric hydroxide (Fe(OH)₃) to help particles enmeshment. Meanwhile, EC/PS also avoids the addition of other anions (Cl⁻ or NO₃⁻) to the treated system, which affects the contaminants degradation [18]. Though EC were known as a practical technique because of its versatility, environmental compatibility, high efficiency and low operation cost, the reported literatures were mainly focused on the combination of EC and Fenton processes [19,20]. Nevertheless, to date little is known about the AO II degradation during the EC/PS process.

Therefore, the objectives of this study are (1) to investigate the performance of AO II degradation in the EC/PS system; (2) to identify the main activated radical species responsible for AO II degradation and (3) to evaluate the influence of the applied current, persulfate concentration, reaction temperature on AO II degradation performance.

2. Materials and methods

2.1. Materials and reagents

All chemicals were of analytical grade except as noted. The solutions were prepared using ultrapure water (18.2 MΩ·cm) from an ELGA purelab water system. Acid Orange II, sodium persulfate (PS, Na₂S₂O₈, ≥99.5%), sodium sulfate (Na₂SO₄, ≥99.0%), ferrous sulfate (FeSO₄·7H₂O, ≥99.0%), tertiary butanol (TBA, ≥98.0%) and methanol (MeOH, ≥99.8%) were obtained from Sinopharm Chemical Reagent Co. (China). All the chemicals were used as-received without further purification.

2.2. Experimental procedures

The stock solution of AO II (500 μM) was prepared before the experiments. The required experimental concentrations of solutions were diluted with ultrapure water when necessary. Na₂S₂O₈ stock solution was freshly prepared immediately prior to use. Batch experiments were conducted in a series of 250-mL borosilicate glass jars. The electrodes with dimensions of 5 cm × 2 cm were set in parallel at a distance of 2 cm, and the total submerged area was 6 cm² (3 cm × 2 cm). A DC source was used to supply the power of the system.

3.0 mM Na₂SO₄ were added to raise the conductivity of the solution. A magnetic stirrer provided mixing of the solution in the reactor. At each designated sampling time, 5.0 mL sample was collected and mixed immediately with appropriate amounts of methanol to quench the residual oxidants. Then, the samples were filtered with 0.45 μm filter membrane before chemical analysis.

2.3. Chemical analysis

The concentrations of AO II were monitored by measuring the absorbency at λ_{max} = 482 nm using a UV-visible spectrophotometer (Hitachi, Japan). The removal rate (η) was calculated from the following expression:

$$\eta(\%) = \frac{A_0 - A_t}{A_0} \times 100\% \quad (3)$$

where A₀ and A_t were the absorbency of the sample at time 0 and time *t*, respectively. The concentrations of Fe²⁺ were determined by spectrophotometric method at 510 nm after complexing with 1,10-phenanthroline.

The intermediates were quantified by liquid/liquid extraction with *n*-hexane followed by a gas chromatography-mass spectrometry (GC-MS; 7890A-5975C, Agilent, USA) using scan mode. The chromatograph was coupled with a HP-5 column (30 m × 0.25 mm, ID = 0.32 μm). The temperature program of oven began at 60°C for 3 min, ramped up to 145°C at 30°C/min, then ramped up to 180°C at 10°C/min and held for 1 min, and finally reached up to 250°C at 40°C/min.

A pH meter (PHS-3G, Leica Corp., China) equipped with a pH electrode was used to monitor pH. Initial pH was set at 7.0 and adjusted by 0.1 M H₂SO₄ or NaOH. Total organic carbon (TOC) in solutions was measured using a Shimadzu VCSH-ASI TOC analyzer. All the experiments were duplicated at 25°C except for the effect of temperature. All the experiments were conducted at least twice and the average values with the standard deviations (error bars) are presented.

3. Results and discussion

3.1. Removal efficiency of AO II in PS, EC and EC/PS system

Fig. 1 shows the semilogarithmic graphs of [AO II]_t/[AO II]₀ as a function of time by persulfate, electrocoagulation and EC/PS process. The relation between time and ln([AO II]_t/[AO II]₀) remained satisfactory linear (R² > 0.99), where [AO II]_t and [AO II]₀ represents the concentrations of AO II at different reaction time and initial time, respectively. The linear relationship indicated the pseudo-first-order kinetics

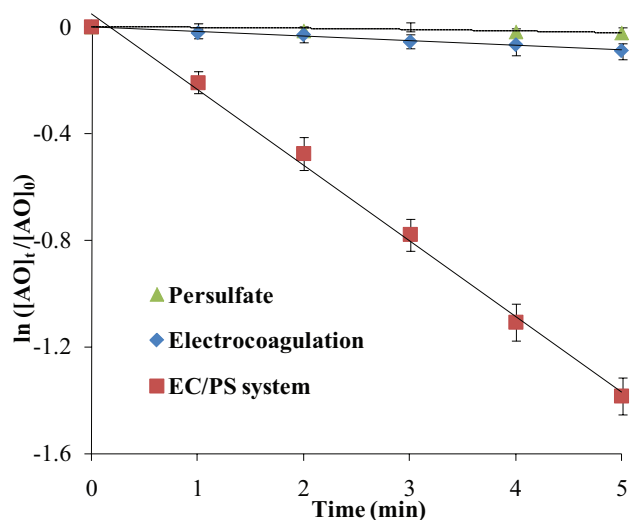


Fig. 1. Comparison of AO II degradation in persulfate, electrocoagulation and EC/PS system. Experimental conditions: applied current = 30 mA, $[AO II]_0 = 50 \mu\text{M}$, $[PS]_0 = 1.0 \text{ mM}$.

with respect to AO II degradation. And the overall rate law for AO II degradation could be expressed as Eq. (4):

$$-d[AO II]/dt = k_{\text{obs}} [AO II] \quad (4)$$

Eq. (4) can be written as:

$$\ln([AO II]_t/[AO II]_0) = -k_{\text{obs}} t \quad (5)$$

where k_{obs} is the pseudo-first-order rate constant (min^{-1}).

As shown in Fig. 1, persulfate and electrocoagulation alone exhibited lower AO II degradation rate compared with the EC/PS system, with approximately 2.0%–8.6% removal at 5 min. However, the addition of 1.0 mM persulfate to the electrocoagulation system significantly improved the degradation performance of AO II, and the removal rate reached up to 75.1% within 5 min. It can be concluded that the EC/PS process is more efficient than persulfate and electrocoagulation process, which may be attributed to the involvement of $\text{SO}_4^{\cdot-}$ activated by the released Fe^{2+} from iron electrode and $\text{HO}\cdot$ generated from the following reaction as Eq. (6). Moreover, the solution pH dropped as the reactions proceeded, and the final pH ranged from 3.8 to 4.1 (Fig. S1 in supplementary information).



3.2. Comparison of AO II removal in the Fe^{2+}/PS and EC/PS system

To further evaluate the removal efficiency of AO II, a comparison between the Fe^{2+}/PS and EC/PS system was conducted in this study. In the Fe^{2+}/PS system, the adding ferrous concentrations were calculated via Faraday's law with a reaction time of 5 min. As shown in Fig. 2(a), unlike the pseudo-first-order reaction in the EC/PS system, the degradation of

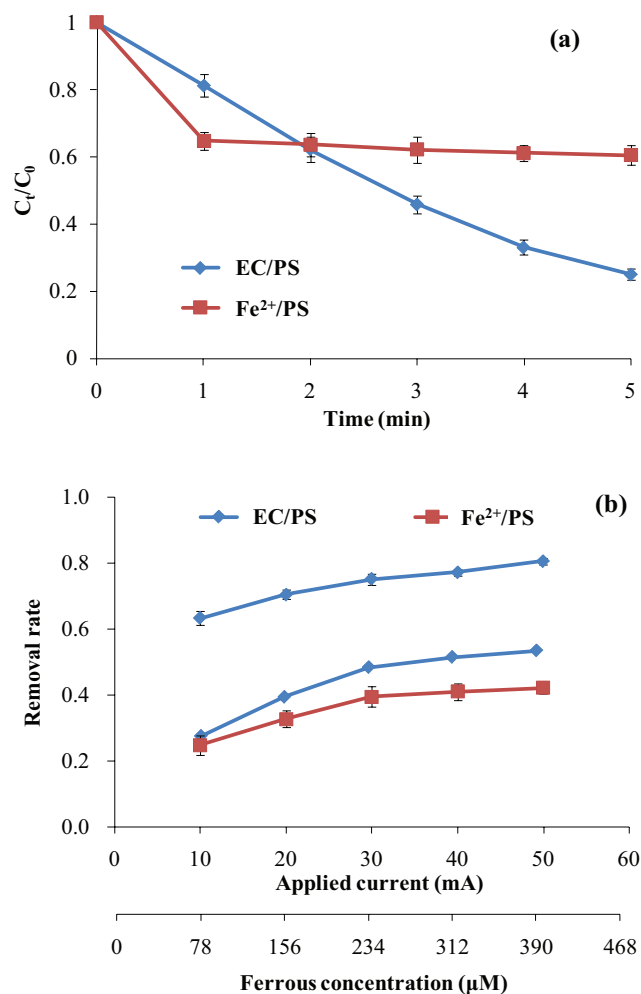


Fig. 2. Comparison of AO II degradation in the EC/PS and Fe^{2+}/PS system. Experimental conditions: (a) applied current = 30 mA, $[\text{Fe}^{2+}]_0 = 234 \mu\text{M}$, (b) applied current = 10–50 mA, $[\text{Fe}^{2+}]_0 = 78$ –390 μM , $[AO II]_0 = 50 \mu\text{M}$, $[PS]_0 = 1.0 \text{ mM}$.

AO II proceeded through a fast stage and then a slow stage in the Fe^{2+}/PS system, which is confirmed by the previous study [21]. Fig. 2(b) also shows that the removal rates of AO II in the EC/PS system were almost twice of those in the Fe^{2+}/PS system at all the applied currents (ferrous concentrations). This phenomenon could be explained as follows. In the Fe^{2+}/PS system, the direct addition of Fe^{2+} can be excess and scavenge the generated $\text{SO}_4^{\cdot-}$ via Eq. (2), thus decreasing the removal rate of AO II. However, the electrochemical activation of persulfate was attributable to the release of Fe^{2+} from the iron electrode. The release rate of Fe^{2+} can be quantitatively controlled by adjusting the applied current, which improved the utilization of Fe^{2+} and persulfate. Therefore, the EC/PS system could remarkably enhance the removal rate of AO II compared with the Fe^{2+}/PS system.

3.3. Contributions of sulfate radical and hydroxyl radical in the EC/PS system

To systematically distinguish the contribution of reactive radical species in the EC/PS system, two radical scavengers,

MeOH and TBA, were used in further experiments. Generally, $\text{SO}_4^{\cdot-}$ are more selective for electron transfer reactions, while OH^{\cdot} can more rapidly undergo hydrogen abstraction or addition reactions [11]. Table 2 shows the second-order rate constants for reactions of selected scavengers with $\text{SO}_4^{\cdot-}$ and OH^{\cdot} . MeOH is an effective quencher for both $\text{SO}_4^{\cdot-}$ and OH^{\cdot} because the reaction rate constant for MeOH reacting with $\text{SO}_4^{\cdot-}$ is similar to that of MeOH reacting with OH^{\cdot} , while TBA is an effect quencher for OH^{\cdot} but not for $\text{SO}_4^{\cdot-}$ because the reaction rate constant of TBA and OH^{\cdot} is much quicker than that of TBA and $\text{SO}_4^{\cdot-}$ [22,23].

As shown in Fig. 3, the coexistence of either MeOH or TBA reduced the rate of AO II degradation, which confirmed that both $\text{SO}_4^{\cdot-}$ and OH^{\cdot} existed in the EC/PS system. Moreover, the pseudo-first-order rate constants k_{obs} decreased slightly by 8.8% with increasing the dosage of TBA from 0 to 200 mM. While the pseudo-first-order rate constants decreased rapidly in the presence of MeOH, and the k_{obs} decreased by 83.3% with increasing the dosage of MeOH from 0 to 200 mM. These results suggested that $\text{SO}_4^{\cdot-}$ is the predominant radical species of AO II degradation in the EC/PS system.

3.4. Effect of applied current

Fig. 4 illustrates the AO II degradation with time at different applied currents during the EC/PS system. The k_{obs} increased from 0.1962 to 0.3372 min^{-1} with increasing the

Table 2
Second-order rate constants for reactions of selected scavengers with sulfate and hydroxyl radicals

Scavengers	Second-order degradation rate constants		References
	Sulfate radicals	Hydroxyl radicals	
TBA	4.0×10^5	6.0×10^8	[22,23]
MeOH	1.1×10^7	9.7×10^8	[22,23]

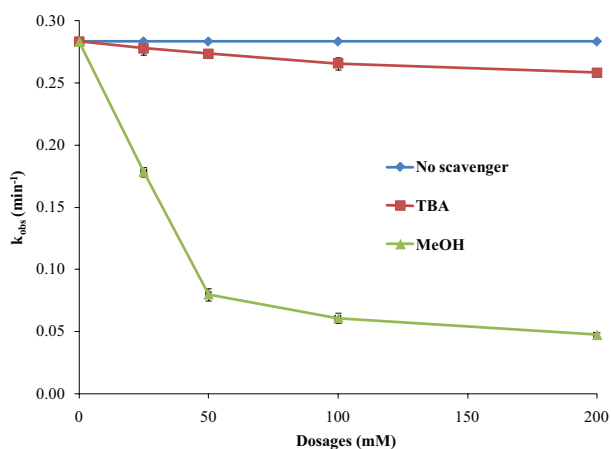


Fig. 3. Effect of coexisting TBA or MeOH on the pseudo-first-order rate constants of AO II degradation. Experimental conditions: applied current = 30 mA, $[\text{AO II}]_0 = 50 \mu\text{M}$, $[\text{PS}]_0 = 1.0 \text{ mM}$, $[\text{TBA}] = 0\text{--}200 \text{ mM}$, $[\text{MeOH}] = 0\text{--}200 \text{ mM}$, reaction time = 5 min.

applied current from 10 to 50 mA. Moreover, the degradation rate constants also exhibited a linear trend as a function of the applied currents as shown in the inset of Fig. 4 ($k_{\text{obs}} = 0.003 I_0 + 0.173$, $R^2 = 0.963$). The results indicated that the applied current had important impact on the degradation of AO II and the higher current caused the faster degradation. Increasing the applied current would accelerate the generation of ferrous ions from iron electrode according to the Faraday's law, and then improve the decomposition of the persulfate to generate sulfate radical (Eq. (1)). Though it was reported that excess Fe^{2+} may decrease the removal rate of target contaminants in the Fe^{2+}/PS system via Eq. (2) [24], this phenomenon was not referred in this study. However, the optimal applied current for the successive EC/PS degradation of AO II may need to be further studied considering the relationship between the removal efficiency and power consumption [25].

3.5. Effect of persulfate concentration

The effect of persulfate concentration on AO II degradation was evaluated by conducting experiments at 0.5, 0.75, 1.0, 1.25 and 1.5 mM, respectively. As shown in Fig. 5, when the persulfate concentration increased from 0.1 to 1.5 mM, the pseudo-first-order rate constants and the removal rates increased from 0.15 to 0.37 min^{-1} and from 52.7% to 83.9%, respectively. Persulfate is a source of sulfate radicals in the EC/PS system via Eq. (1), and more reactive $\text{SO}_4^{\cdot-}$ and OH^{\cdot} (Eq. (6)) would be generated to degrade AO II at higher persulfate concentration. However, excess persulfate can also scavenge $\text{SO}_4^{\cdot-}$ and OH^{\cdot} via Eqs. (7) and (8). Therefore, the removal rate of AO II increased less rapidly at persulfate concentration of 1.0 mM or above, as observed in Fig. 5(b). According to the obtained results, 1.0 mM was chosen as the optimal persulfate concentration value and used in this study.

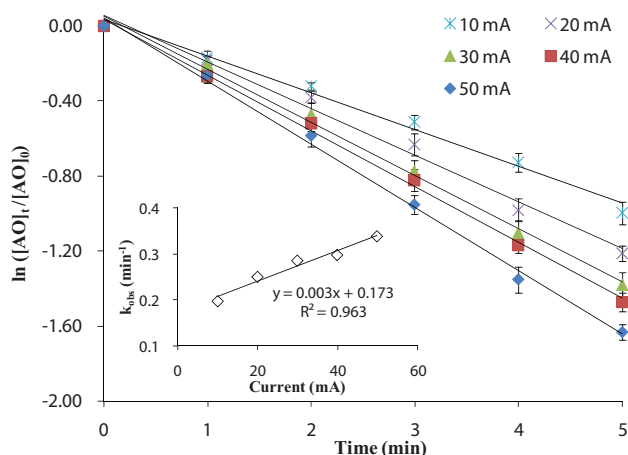
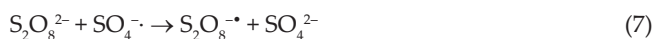


Fig. 4. Effect of applied current on the degradation of AO II in the EC/PS system. Experimental conditions: $[\text{AO II}]_0 = 50 \mu\text{M}$, $[\text{PS}]_0 = 1.0 \text{ mM}$.

3.6. Effect of reaction temperature

The effect of reaction temperature (15°C–45°C) on the degradation of AO II in the EC/PS system was investigated as shown in Fig. 6, where AO II degradation increased as

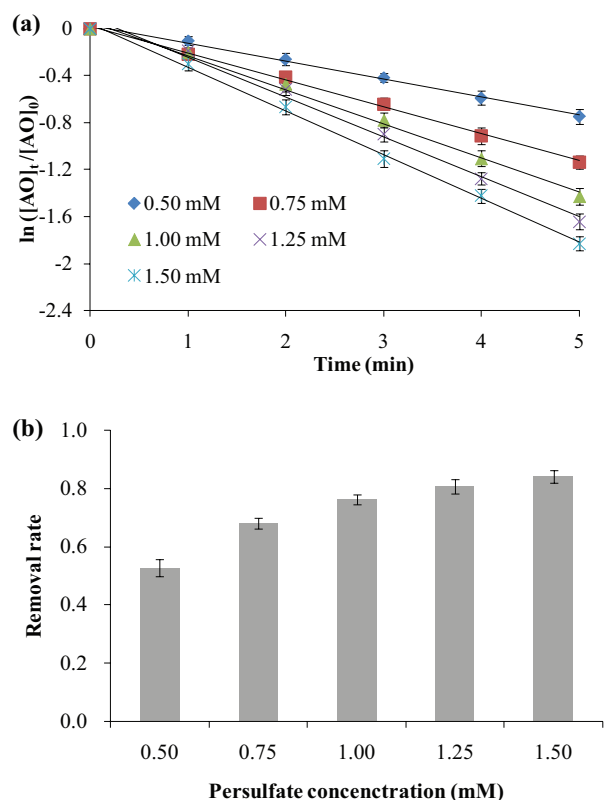


Fig. 5. Effect of persulfate concentration on the pseudo-first-order constants and removal rates of AO II in the EC/PS system. Experimental conditions: applied current = 30 mA, $[AO II]_0 = 50 \mu\text{M}$.

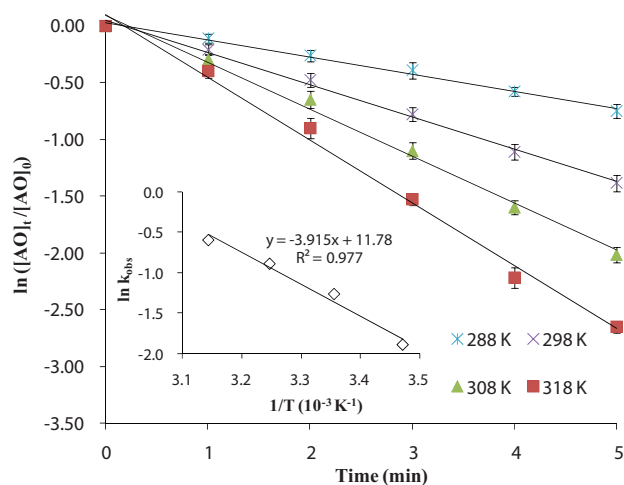


Fig. 6. Effect of reaction temperature on the degradation of AO II in the EC/PS system. Experimental conditions: applied current = 30 mA, $[AO II]_0 = 50 \mu\text{M}$, $[PS]_0 = 1.0 \text{mM}$.

temperature increased. The pseudo-first-order rate constants increased from 0.15min^{-1} at 15°C to 0.28, 0.41 and 0.55min^{-1} for 25°C, 35°C and 45°C within 5 min, respectively. It indicated that more reactive species ($\text{SO}_4^{\cdot-}$ or OH^{\cdot}) were generated in the EC/PS system due to the activation of persulfate by heat and more ferrous. The activation energy (E_a) of AO II degradation was determined by plotting $\ln k_{obs}$ against $1/T$, according to the Arrhenius equation in the following Eq. (9):

$$\ln k_{obs} = \ln A - \frac{E_a}{RT} \quad (9)$$

where A is the Arrhenius constant; E_a is the activation energy (kJ mol^{-1}); R is the universal gas constant ($8.314 \times 10^{-3} \text{kJ (mol K}^{-1})$); T is the absolute temperature (K). The Arrhenius type model implies that increased temperature can accelerate the reaction rate. As shown in the inset of Fig. 6, a clear linear relationship was obtained in the Arrhenius plot of $\ln k_{obs}$ vs. $1/T$. The activation energy (E_a) calculated through the slope was 32.6kJ mol^{-1} , which is lower than the value of 92.2kJ mol^{-1} required for azo dye Orange G degradation in the Fe^{2+}/PS system [26]. Actually, the degradation of AO II in the EC/PS system can be easily achieved, as the thermal reaction energy has a normal range of 60–250 kJ mol^{-1} [26,27].

3.7. Proposed pathway of AO II degradation and mineralization

In order to obtain the qualitative information about the degradation of AO II in the EC/PS system, a set of representative UV–visible spectra are presented in Fig. 7. The UV–visible spectra of AO II display four main transitions: one in the visible region at 482 nm ($-\text{N}=\text{N}-$), and three transitions in the ultraviolet region at 230, 255 and 311 nm [28]. The characteristic adsorption peak at 482 nm, used to measure the decolorization of the dye solution, can be attributed to the chromophore group ($-\text{N}=\text{N}-$). The adsorption peaks in the ultraviolet region (below 400 nm) are assigned to the aromatic rings (e.g., benzene ring, naphthalene ring and their derivatives).

As shown in Fig. 7, the adsorption peak at 487 nm decreased quickly with the reaction evolution, indicating that the double bonded nitrogen in the dye was destroyed efficiently. Meanwhile, the intensity of the peak at 487 nm decreased more and more completely as the applied currents increased. This means that the azo double bond in the degradation of AO II is probably under current control in the EC/PS system, well approving the discussions in section 3.4. Furthermore, it is clearly observed that the adsorption peak at 254 nm, corresponding to phenol in the AO II structure, appeared and increased with the extension of the reaction time. The result is consistent with the finding of other studies that some intermediates such as phenols or benzenes did not disappear and accumulated within reaction time in the electrooxidation of AO II [29], and the benzene molecules may be released from the breaking of the C–N single bond between azo group and benzene ring [30].

Furthermore, the main intermediate products of AO II were determined using a GC–MS analyzer as shown in Fig. S2 in supplementary information. Based on the results and previous studies, a plausible pathway for AO II degradation in the EC/PS system was proposed in Fig. 8. As shown,

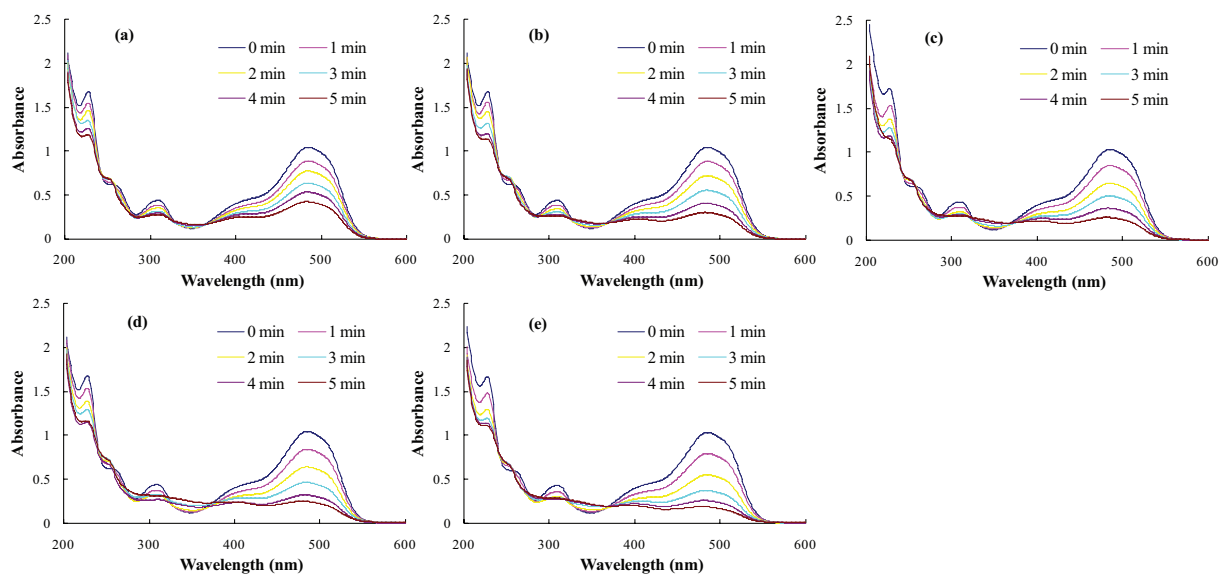


Fig. 7. UV-visible absorbance variation of AO II degradation under different applied currents in the EC/PS system. (a) 10 mA, (b) 20 mA, (c) 30 mA, (d) 40 mA and (e) 50 mA.

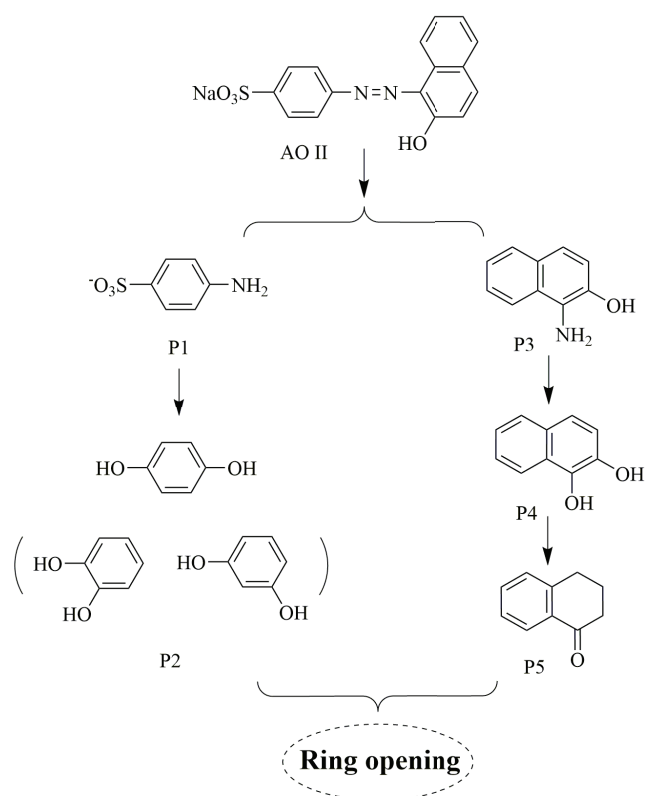


Fig. 8. Proposed pathway for AO II degradation in the EC/PS system.

the radicals attacked N=N bonds first, then the cleavage of N=N leads to the formation of sodium sulfanilamide (P1) and 1-amino-2-naphthol (P3). The further degradation of P1 caused by radicals gave rise to the production of P2. And P4 could be formed via electron transfer reaction, which

was subsequently oxidized to generate P5. All the organics would be transformed to organics with small molecular weight via a ring opening reaction and finally mineralized to CO₂ and H₂O. Therefore, the mineralization degree of AO II during the EC/PS system was calculated from TOC values (Fig. S3 in supplementary information). Although the removal rate of AO II reached up to 75.1% within 5 min, the specific TOC removal increased from 0% to 12.9%, indicating that most of the degraded AO II remains in the solution as decomposition intermediates, and further oxidation are needed.

4. Conclusion

In this present work, iron anode was employed to activate persulfate to degrade a typical azo dye (AO II) and the following conclusions can be drawn:

- The EC/PS system presented higher efficiency to degrade AO II than persulfate oxidation, electrocoagulation and Fe²⁺/PS system.
- Both SO₄⁻ and OH[·] existed in the EC/PS system and SO₄⁻ is the predominant radical species for AO II degradation.
- Higher applied current, persulfate concentration and reaction temperature are favorable for the removal of AO II.
- The results of UV-visible spectra demonstrated that the azo double bond in the AO II structure was destroyed efficiently. Five intermediates were identified and a probable pathway of AO II degradation was proposed.

Acknowledgment

This work was financially supported by the National Major Project of Science and Technology Ministry of China (Nos. 2012ZX07403-001; 2012ZX07403-002 and 2008ZX07421-002).

References

- [1] H. Lin, H. Zhang, X. Wang, L.G. Wang, J. Wu, Electro-Fenton removal of Orange II in a divided cell: reaction mechanism, degradation pathway and toxicity evolution, *Sep. Purif. Technol.*, 122 (2014) 533–540.
- [2] M. Kousha, E. Daneshvar, M.S. Sohrabi, M. Jokar, A. Bhatnagar, Adsorption of acid orange II dye by raw and chemically modified brown macroalga *Stoichospermum marginatum*, *Chem. Eng. J.*, 192 (2012) 67–76.
- [3] Y. Bessekhouad, N. Chaoui, M. Trzpit, N. Ghazzal, D. Robert, J. Weber, UV–vis versus visible degradation of Acid Orange II in a coupled CdS/TiO₂ semiconductors suspension, *J. Photochem. Photobiol., A*, 183 (2006) 218–224.
- [4] N. Daneshvar, H. Ashassi-Sorkhabi, A. Tizpar, Decolorization of orange II by electrocoagulation method, *Sep. Purif. Technol.*, 31 (2003) 153–162.
- [5] E.N. El Qada, S.J. Allen, G.M. Walker, Adsorption of basic dyes from aqueous solution onto activated carbons, *Chem. Eng. J.*, 135 (2008) 174–184.
- [6] M.S. Khehra, H.S. Saini, D.K. Sharma, B.S. Chadha, S.S. Chimni, Biodegradation of azo dye CI Acid Red 88 by an anoxic–aerobic sequential bioreactor, *Dyes Pigm.*, 70 (2006) 1–7.
- [7] S.P. Sun, C.J. Li, J.H. Sun, S.H. Shi, M.H. Fan, Q. Zhou, Decolorization of an azo dye Orange G in aqueous solution by Fenton oxidation process: effect of system parameters and kinetic study, *J. Hazard. Mater.*, 161 (2009) 1052–1057.
- [8] S. Papić, I. Peternel, Ž. Krevzelj, H. Kušić, N. Koprivanac, Advanced oxidation of an azo dye and its synthesis intermediates in aqueous solution: effect of Fenton treatment on mineralization, biodegradability and toxicity, *Environ. Eng. Manage. J.*, 13 (2014) 2561–2571.
- [9] J.Z. Mitrović, M.D. Radović, T.D. Anđelković, D.V. Bojić, A.L. Bojić, Identification of intermediates and ecotoxicity assessment during the UV/H₂O₂ oxidation of azo dye Reactive Orange 16, *J. Environ. Sci. Health, Part A*, 49 (2014) 491–502.
- [10] O.S. Furman, A.L. Teel, R.J. Watts, Mechanism of base activation of persulfate, *Environ. Sci. Technol.*, 44 (2010) 6423–6428.
- [11] G.P. Anipsitakis, D.D. Dionysiou, Radical generation by the interaction of transition metals with common oxidants, *Environ. Sci. Technol.*, 38 (2004) 3705–3712.
- [12] C.J. Liang, C.J. Bruell, Thermally activated persulfate oxidation of trichloroethylene: experimental investigation of reaction orders, *Ind. Eng. Chem. Res.*, 47 (2008) 2912–2918.
- [13] X.G. Gu, S.G. Lu, Z.F. Qiu, Q. Su, C.J. Banks, T. Imai, K.F. Lin, Q.S. Luo, Photodegradation performance of 1,1,1-trichloroethane in aqueous solution: in the presence and absence of persulfate, *Chem. Eng. J.*, 215 (2013) 29–35.
- [14] F.F. Hao, L.L. Guo, A.Q. Wang, Y.Q. Leng, H.L. Li, Intensification of sonochemical degradation of ammonium perfluorooctanoate by persulfate oxidant, *Ultrason. Sonochem.*, 21 (2014) 554–558.
- [15] C.J. Liang, C.J. Bruell, M.C. Marley, K.L. Sperry, Persulfate oxidation for in situ remediation of TCE. I. Activated by ferrous ion with and without a persulfate–thiosulfate redox couple, *Chemosphere*, 55 (2004) 1213–1223.
- [16] D.A. House, Kinetics and mechanism of oxidations by peroxydisulfate, *Chem. Rev.*, 62 (1962) 185–203.
- [17] J.Y. Zhao, Y.B. Zhang, X. Quan, S. Chen, Enhanced oxidation of 4-chlorophenol using sulfate radicals generated from zero-valent iron and peroxydisulfate at ambient temperature, *Sep. Purif. Technol.*, 71 (2010) 302–307.
- [18] C. Tan, N. Gao, Y. Deng, Y. Zhang, M. Sui, J. Deng, S. Zhou, Degradation of antipyrine by UV, UV/H₂O₂ and UV/PS, *J. Hazard. Mater.*, 260 (2013) 1008–1016.
- [19] F. Almomani, E.A. Baranova, Kinetic study of electro-Fenton oxidation of azo dyes on boron-doped diamond electrode, *Environ. Technol.*, 34 (2013) 1473–1479.
- [20] A. Akyol, O.T. Can, E. Demirbas, M. Kobya, A comparative study of electrocoagulation and electro-Fenton for treatment of wastewater from liquid organic fertilizer plant, *Sep. Purif. Technol.*, 112 (2013) 11–19.
- [21] C. Tan, N. Gao, W. Chu, C. Li, M.R. Templeton, Degradation of diuron by persulfate activated with ferrous ion, *Sep. Purif. Technol.*, 95 (2012) 44–48.
- [22] P. Neta, R.E. Huie, A.B. Ross, Rate constants for reactions of inorganic radicals in aqueous solution, *J. Phys. Chem. Ref. Data*, 17 (1988) 1027–1284.
- [23] G.V. Buxton, C.L. Greenstock, W.P. Helman, A.B. Ross, Critical review of rate constants for reactions of hydrated electrons, hydrogen atoms and hydroxyl radicals (·OH/·O⁻ in aqueous solution), *J. Phys. Chem. Ref. Data*, 17 (1988) 513–886.
- [24] A. Rastogi, S.R. Al-Abed, D.D. Dionysiou, Effect of inorganic, synthetic and naturally occurring chelating agents on Fe(II) mediated advanced oxidation of chlorophenols, *Water Res.*, 43 (2009) 684–694.
- [25] L. Yue, J. Guo, J. Yang, J. Lian, X. Luo, X. Wang, K. Wang, L. Wang, Studies on the electrochemical degradation of Acid Orange II wastewater with cathodes modified by quinones, *J. Ind. Eng. Chem.*, 20 (2014) 752–758.
- [26] X.-R. Xu, X.-Z. Li, Degradation of azo dye Orange G in aqueous solutions by persulfate with ferrous ion, *Sep. Purif. Technol.*, 72 (2010) 105–111.
- [27] R. Li, X. Jin, M. Megharaj, R. Naidu, Z. Chen, Heterogeneous Fenton oxidation of 2,4-dichlorophenol using iron-based nanoparticles and persulfate system, *Chem. Eng. J.*, 264 (2015) 587–594.
- [28] C. Zhang, L. Liu, W. Li, J. Wu, F. Rong, D. Fu, Electrochemical degradation of Acid Orange II dye with boron-doped diamond electrode: role of operating parameters in the absence and in the presence of NaCl, *J. Electroanal. Chem.*, 726 (2014) 77–83.
- [29] J. Qu, X. Zhao, Design of BDD–TiO₂ hybrid electrode with P–N junction for photoelectrocatalytic degradation of organic contaminants, *Environ. Sci. Technol.*, 42 (2008) 4934–4939.
- [30] J.T. Spadaro, L. Isabelle, V. Renganathan, Hydroxyl radical mediated degradation of azo dyes: evidence for benzene generation, *Environ. Sci. Technol.*, 28 (1994) 1389–1393.

Supplementary information

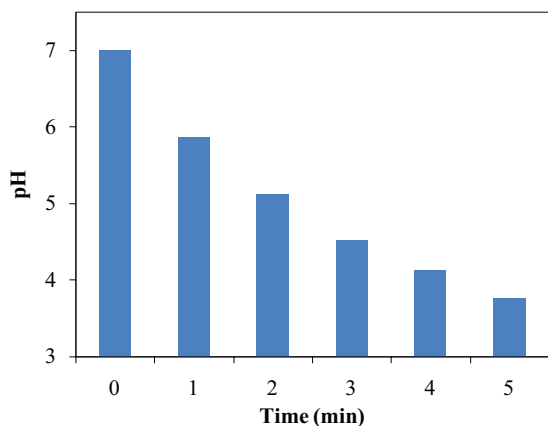


Fig. S1. Variation of pH values in the degradation of AO II during the EC/PS system. Experimental conditions: applied current = 30 mA, $[AO II]_0 = 50 \mu M$, $[PS]_0 = 1.0 \text{ mM}$ and initial pH = 7.0.

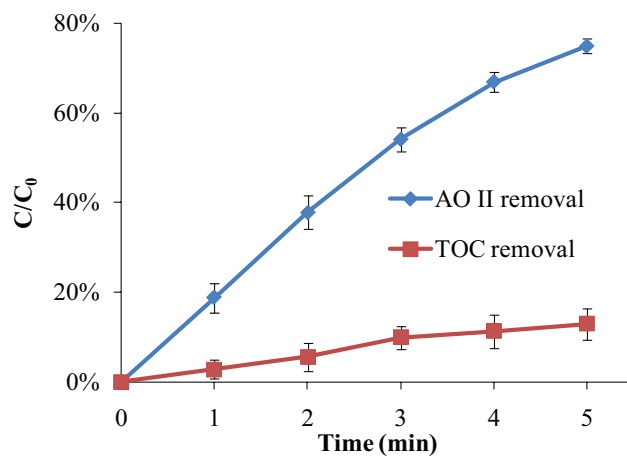


Fig. S3. Changes of AO II removal rate and TOC removal rate during the EC/PS system. Experimental conditions: applied current = 30 mA, $[AO II]_0 = 50 \mu M$, $[PS]_0 = 1.0 \text{ mM}$.

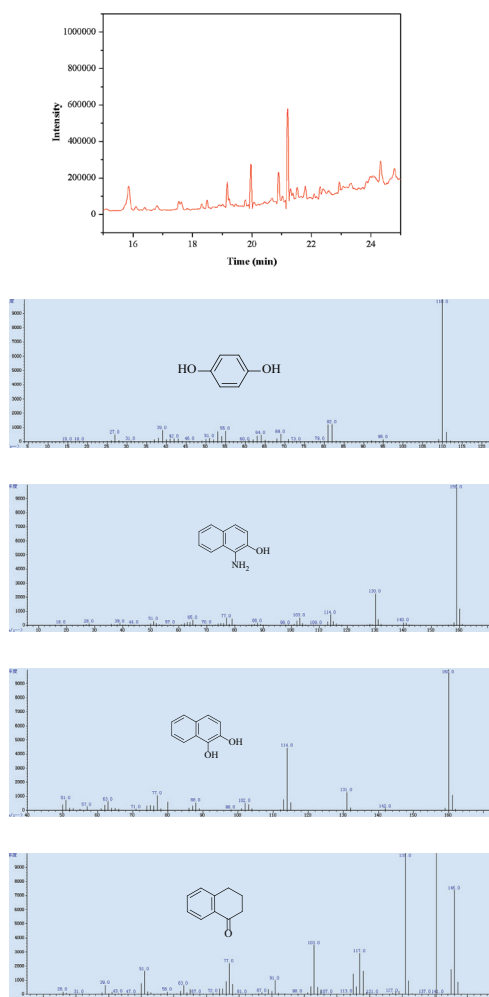


Fig. S2. Gas chromatography–mass spectrometry and mass spectrum of different AO II intermediates.